Mesoscale Temperature Fluctuations and Polar Stratospheric Clouds

D. M. MURPHY

Aeronomy Laboratory, NOAA, Boulder, Colorado

B. L. GARY

Jet Propulsion Laboratory, California Institute of Technology, Pasadena, California

(Manuscript received 17 May 1994, in final form 22 November 1994)

ABSTRACT

Remote sensing measurements of temperature fluctuations on isentropic surfaces, as well as in situ measurements, are used to show that even high-resolution trajectory calculations seriously underestimate the rate of change of temperature experienced by air parcels. Rapid temperature fluctuations will affect the nucleation of polar stratospheric cloud (PSC) droplets and could promote the formation of metastable phases in PSCs. Mesoscale temperature fluctuations are large enough to produce significant departures from equilibrium in established PSCs. The large cooling rates experienced by air parcels have important implications for denitrification and dehydration: nearly all condensation nuclei should be activated when a PSC is first formed and mass must be redistributed to larger aerosols during the evolution of a PSC if denitrification is to occur.

1. Introduction

Polar stratospheric clouds (PSCs) are important to stratospheric chemistry, especially the chemistry involved in polar ozone depletion. PSCs are usually grouped into two categories: type I PSCs occur at temperatures colder than the condensation point of nitric acid trihydrate (NAT); the condensed material corresponds to parts per billion in the gas phase and consists of NAT, other phases of nitric acid, water, and possibly other species. Type II PSCs occur at temperatures colder than the frost point; the condensed material corresponds to parts per million in the gas phase and consists mostly of ice. This paper discusses the impact of mesoscale temperature fluctuations on the nucleation and evolution of both type I and type II PSCs.

The nucleation of PSCs depends on the rate of change of temperature, as well as on the temperature itself (Toon et al. 1989; Salawitch et al. 1989; Drdla and Turco 1991). A rapid temperature reduction as an air parcel cools across the threshold for forming a PSC will favor nucleation on all existing particles, while a slow temperature reduction will favor the growth of only the larger preexisting particles. We show here that the rate of change of temperature is seriously underestimated by trajectory calculations. In fact, the rate of change of temperature is strongly influenced by fluctuations on scales smaller than 10 km. In contrast to the *rate* of temperature change, trajectory calculations do reproduce most of the *magnitude* of temperature fluctuations, except in mountain wave events.

The supersaturations produced by temperature fluctuations faster than a characteristic relaxation time are much larger than the supersaturations produced by slower fluctuations. Using high spatial resolution temperature measurements along with scaling laws, we show that rapid temperature fluctuations produce large supersaturations even though the temperature changes are fairly small. Although a full microphysical model will be necessary to quantify the effects of mesoscale fluctuations on denitrification and dehydration, the brief treatment presented here demonstrates that small but rapid temperature fluctuations could alter the evolution of a PSC.

2. Temperature profiler measurements

Mesoscale temperature fluctuations in the lower stratosphere have been measured by the microwave temperature profiler (MTP) aboard the NASA ER-2 aircraft. The MTP measures the air temperature over an altitude region extending from approximately 2 km below to 3 km above the aircraft (Denning et al. 1989). Excellent measured correlations during dives and ascents between the temperatures derived from MTP data and in situ temperatures give a very high degree of confidence that the MTP data accurately represent air temperatures above and below the airplane.

The measured temperature profiles can be converted to cross sections showing the altitude of potential tem-

Corresponding author address: Dr. Daniel M. Murphy, NOAA Aeronomy Laboratory, 325 Broadway, Boulder, CO 80303.

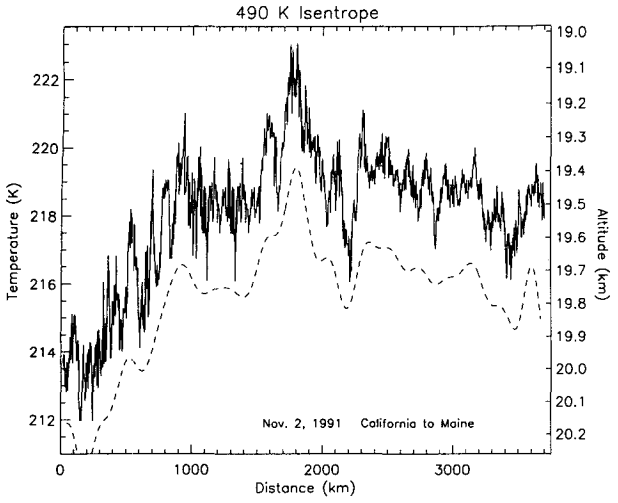

FIG. 1. Temperature of the 490-K isentrope measured by the microwave temperature profiler from the ER-2 on 2 November 1991 using a horizontal resolution of 5 km. The finestructure is due to small-scale waves, not instrument noise. The right-hand scale shows the corresponding altitude of the isentrope. The data smoothed to include wavelengths longer than 200 km are also shown (dashed line; displaced 3 K for clarity). Although the smoothed data preserve the magnitude of the temperature fluctuations, they do not capture the rate of change. For these data, $|dT/dt|$ is over 200 K day^{-1} at full resolution and 23 K day^{-1} when smoothed.

perature surfaces. If the ER-2 is flying parallel to the wind, then such cross sections represent the actual altitude and hence temperature excursions experienced by air parcels undergoing adiabatic heating and cooling. Figure 1 shows an example of MTP data for an ER-2 flight from California to Maine. Typical wave amplitudes are 0.8 K over water and 1.6 K over land at altitudes near 20 km (Gary 1989; Bacmeister and Gary 1990).

It is evident in examples such as Fig. 1 that the heating and cooling rates are much larger in the finely resolved data than for the curve, which is smoothed to the resolution of typical trajectory calculations. For the data in Fig. 1, the mean absolute value of the cooling rate is >200 K day^{-1} for the data at full resolution, ~23 K day^{-1} when smoothed to 200-km resolution, and ~12 K day^{-1} when smoothed to 400-km resolution.

3. Power spectra

The spectral density of measured temperatures shows the importance of small scales to the rate of change of temperature. Since mesoscale motions in the stratosphere are approximately isentropic, the desired quantity for computing temperature fluctuations is the spectral density of temperature at constant potential temperature. Except for the limited amount of MTP data used here, we are not aware of any high-resolution datasets of temperature at constant potential temperature. The Global Atmospheric Sampling Program (GASP) provided one of the most extensive sets of data for computing spectral densities (Gage and Nastrom 1986; Nastrom et al. 1986). GASP spectral densities are available for potential temperature fluctuations along the flight paths of commercial airliners. Since airliners fly at approximately constant pressure during flight legs, the measured spectra of potential temperature are approximately equal to the spectra of temperature at constant pressure, except for a scale factor $[(1000/p)^{0.286}]^2$ where p is the flight pressure in millibars.

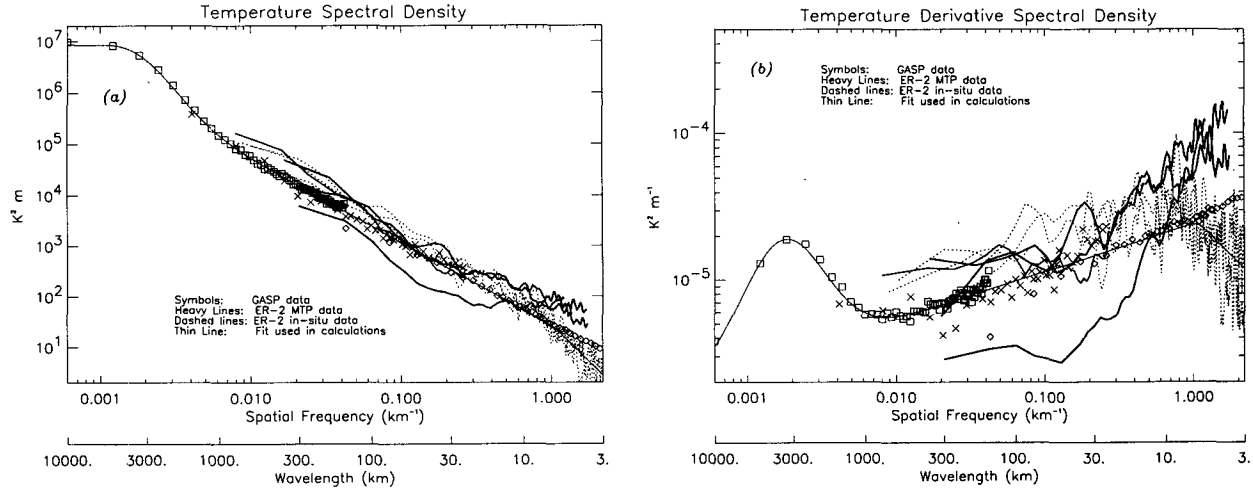

FIG. 2. (a) Spectral density of observed temperature fluctuations for the GASP data (symbols), MTP data on the ER-2 (solid lines), and ER-2 in situ data (dashed lines). A fit to the GASP data at low frequencies and the ER-2 in situ data at high frequencies is also shown (thin line). (b) Spectral density of the spatial derivative of temperature fluctuations. MTP data are from flights 881231, 890221, 911102, and two legs of 940204. In situ data are from flights 881231, 890220, and 890221.

TABLE 1. Temperature fluctuations by length scale. Contributions from more than one range should be added as the square root of the sum of squares.

	Wavenumber range			
	0.0004–0.01 km^{-1}	0.01–0.04 km^{-1}	0.04–0.1 km^{-1}	0.1–0.4 km^{-1}
Temp. fluctuation	4.2 K	0.7 K	0.4 K	0.3 K
Rate of change	19 K day^{-1}	30 K day^{-1}	51 K day^{-1}	140 K day^{-1}

Figure 2 shows the spectral density of temperature fluctuations versus length scale for the MTP and GASP data. Also shown in Fig. 2 are spectra of in situ temperature measured on the ER-2 for three east–west flights (Scott et al. 1990). There is agreement between the GASP and ER-2 data in spite of different flight altitudes (9–14 and 18–21 km, respectively). The spectral densities of temperature at constant pressure (as in the GASP data) are not necessarily equal to the spectral densities at constant potential temperature (as in the MTP data). However, the spectral densities in Fig. 2 are similar for all three methods, lending some confidence that GASP data can be used to supplement the ER-2 data. The ER-2 in situ data fall off more rapidly at high frequencies than the other data. It is not clear whether this is a real difference or an instrumental effect. A small amount of noise in the MTP and GASP data could account for the difference. Aircraft "bobbing" may also affect the high-frequency end of the spectrum. A more detailed treatment of the MTP-based spectral densities is underway.

Two general properties of spectral densities are of interest here. First, the integral of the spectral density Φ between two frequencies is equal to the contribution of those frequencies to the variance of the data. Second, the spectral density of the time derivative of a time-varying signal is just $\omega^2\Phi$, where ω is the frequency (Tolstov 1962). The abscissa of Fig. 2 can be converted between wavenumber and angular frequency by using the wind speed. A consequence of the derivative property is that small scales dominate the rate of change of temperature if the slope of the spectral density of temperature fluctuations is greater than -2, whereas large scales dominate if the slope is less than -2. A variety of data shows that atmospheric spectral densities in the lower stratosphere have slopes between -1.6 and -3, with slopes commonly near $-5/3$ at horizontal scales of less than 800 km (Gage and Nastrom 1986; Murphy 1989; B. Gary, unpublished data). Slopes near -2 would imply that *all* spatial scales contribute significantly to the rate of change of temperature for air parcels.

Figure 2b shows the spectral density of the spatial derivative $k^2\Phi$, where k is the spatial frequency. The spectral density of the derivative shows a clear peak at synoptic scales. A wind speed u is needed to transform $k^2\Phi$, the spectrum of the spatial derivative, to $\omega^2\Phi = k^2u^2\Phi$, the spectrum of the time derivative. An average wind speed of 24 m s^{-1} is used for the GASP data (Nastrom and Gage 1985). Average observed winds for each flight leg, ranging from 19 to 50 m s^{-1}, are used for the ER-2 data. By integrating under the spectra in Fig. 2, we obtain estimates of the mean fluctuations of the temperature and the derivative. Results are shown in Table 1. Most of the rate of change of temperature comes from wavenumbers above 0.1 km^{-1} or wavelengths of less than 60 km.

Trajectory calculations using operational meteorology models will reproduce temperature fluctuations up to the highest spatial scale resolved by the model. A very high resolution (T213) model can resolve spatial frequencies $k \approx 2\pi/\lambda$ up to about 0.06 km^{-1} (Laprise 1992) and a lower-resolution model with 100-km grid spacing up to $k \approx 0.03$ km^{-1}. The actual frequency limit will be less because numerical models are strongly damped near their upper frequency limits. Table 1 shows that although a trajectory based on an operational model can capture most of the magnitude of the temperature fluctuations, such trajectories do not reproduce the instantaneous rates of cooling and heating shown by the observations. The observed rates of temperature change are much faster than even the fastest temperature oscillations in Drdla and Turco (1991), whose scenarios covered oscillations with periods of 1 to 5 days.

4. Cooling rates during PSC formation

The microphysics of aerosols sets the range of frequencies to be considered in plots like those in Fig. 2. Two time constants are of interest for PSCs: the time to significantly change particle diameters and the time to add or significantly change the partial pressure of the condensing species. A simplified mass transfer equation is

$$dm/dt \approx 4\pi aD\beta\rho_\Delta, \qquad (1)$$

where m is the mass of a single aerosol particle of radius a, D is the diffusion constant of the condensing species, $\beta = 1/(1 + 4Kn/3)$ is the transitional correction factor of the Knudsen number Kn, and $\rho_\Delta = (p\xi - p_v)M/RT$ is the density difference between the partial pressure and vapor pressure of the condensing species. At PSC conditions, Eq. (1) is accurate to about 20% compared with a full treatment of mass transfer (Wagner 1982). If ρ_Δ is approximately constant, then

TABLE 2. Sample time constants for mass transfer.

			Forming PSCs						
	T K	N cm^{-3}	a μm	Condensed[a]	s[b]	τ_g min	λ_g[c] km	τ_p min	$\overline{\lvert dT/dt \rvert}$ K day^{-1}
Type I	194.1	8	0.2	0.6 ppbv	0.8 (2.4 ppbv)	68	86	60	50
Type II	188.0	4	0.9	0.2 ppmv	0.04 (0.2 ppmv)	5	7	7	>100

			Established PSCs				
	T K	N cm^{-3}	a μm	Condensed[a]	τ_g min	λ_g[c] km	$\overline{\lvert s \rvert}$
Type I	193.1	8	0.35	4.2 ppbv	23	33	0.45 (0.8 ppbv)
Type I	191.0	8	0.37	5.5 ppbv	21	30	0.45 (0.2 ppbv)
Type II	185.4	4	2.0	2.0 ppmv	1.3	2	0.035 (0.1 ppmv)

[a] Amount of gas-phase HNO_3 (type I PSCs) or H_2O (type II PSCs) condensed onto the paticles as derived from number and radius assuming a 0.1-μm radius nonvolatile core.

[b] Here s is the supersaturation expressed as a fraction. The number in parentheses is the amount of gas-phase HNO_3 (type I PSCs) or H_2O (type II PSCs) corresponding to that supersaturation.

[c] Assuming a wind speed of 24 m s^{-1}.

All calculations at 50 mbar.

the equation for the change in radius of a sphere $da/dt = (dV/dt)(1/4\pi a^2)$ may be integrated to give the time constant for an aerosol particle to grow in radius by $\sqrt{2}$ or evaporate completely. The result is

$$\tau_p = 2\pi a^3 \rho_p/(dm/dt) \approx a^2 \rho_p / 2D\beta\rho_\Delta, \quad (2)$$

where ρ_p is the density of the particle. Conversely, if a and the temperature are approximately constant, then the partial pressure will relax exponentially to the vapor pressure with a time constant

$$\tau_g = \rho_\Delta/(N(dm/dt)) \approx 1/(4\pi a D\beta N), \quad (3)$$

where N is the number density of aerosol particles. Qualitatively, τ_p and τ_g show that when particles are small, they grow quickly in a proportional sense, but gas-phase concentrations change slowly. When the departures from equilibrium ρ_Δ are large, particles grow or evaporate quickly, but the gas-phase time constant is unaffected until the particles change size. If τ_p and τ_g are comparable, then the partial pressure of the condensing species and the aerosol size change simultaneously in a more complicated manner.

We separate a discussion of τ_p and τ_g into timescales appropriate to PSCs as they start to form and once the PSCs are established. The equilibration of water in type I PSCs is much faster than the equilibration of nitric acid because the partial pressure of water is much greater than that of nitric acid. Therefore, all references to characteristic times and supersaturations in this paper for type I PSCs refer to nitric acid. Growing aerosol particles will essentially integrate out temperature fluctuations on timescales much shorter than τ_p. Therefore, the initial size distribution of a PSC will be determined by the cooling rate over a time of order τ_p after the condensation point is reached. Substituting into Eq. (2) for a forming type I PSC with ρ_Δ equivalent to 2.4 ppbv of HNO_3, p = 50 mbar, and a = 0.2 μm, we find that τ_p is about 60 min, using a diffusion coefficient for nitric acid $D \approx (0.0077/p)(T/200)^{1.75}$ m^2 s^{-1}, where p is in millibars. At a wind speed of 24 m s^{-1} the maximum spatial frequency corresponding to $\tau_p \approx 60$ min is about 0.07 km^{-1}; the corresponding rate of temperature change due to all larger spatial scales is greater than 50 K day^{-1} (Table 1). The assumed wind speed partially cancels out of this derivation: a higher wind speed implies a smaller maximum spatial frequency but a higher cooling rate for a given spatial frequency. For a spectral density Φ that varies as k^{-2} the cooling rate scales as $(u)^{1/2}$.

An analogous calculation for a forming type II PSC with ρ_Δ equivalent to 0.2 ppmv of H_2O and a = 0.9 μm yields $\tau_p \approx 7$ min. For both PSC cases, τ_p and τ_g are comparable so that the supersaturation and aerosol size change simultaneously. This complicates the interpretation of the rate of temperature change over the period τ_p but will not alter the conclusion that typical cooling rates are >50 K day^{-1} over the time it takes to establish the initial size distribution.

5. Supersaturation in established PSCs

The time constants τ_p and τ_g are very different for an established PSC than they are during the initial condensation. Using Eq. (3), τ_g is about 23 min for a type I PSC with N = 8 cm^{-3} and a = 0.35 μm. For a type II PSC with N = 4 cm^{-3} and a = 2 μm, τ_g is about 80 s. In both cases, $\tau_p \gg \tau_g$; that is, the gas-phase responses are quicker than the particle size changes. This is due to the increased surface area in an established PSC and the reduced amount of gas-phase material

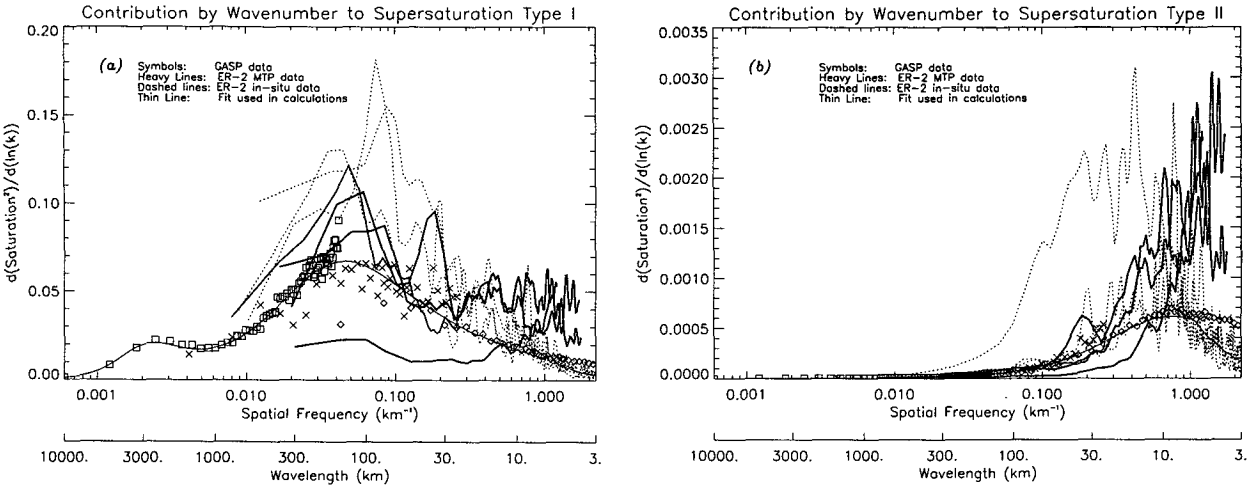

FIG. 3. Contribution to the variance of supersaturations by wavenumber for the GASP data (symbols), MTP data on the ER-2 (solid lines), and ER-2 in situ data (dashed lines). The plot is of $k\Phi_S$ so that the variance of the supersaturation is proportional to the visual area under the curve. These data were not taken in PSCs but rather represent the supersaturation in a PSC for representative temperature fluctuations. (a) Type I PSC conditions. (b) Type II PSC conditions.

present after condensation. Timescales for both forming and established PSCs are shown in Table 2.

Over times much larger than τ_g, the gas will have time to respond to the temperature by condensing onto or evaporating from the particles. For times less than τ_g the gas phase cannot stay in equilibrium with the particles. We define $|\Delta T|_g$ as the typical temperature fluctuation over timescales less than τ_g. By integrating from the right in Fig. 2a or Table 1 we obtain $|\Delta T|_g \approx 0.6$ K for the type I PSC conditions and $|\Delta T|_g \approx 0.2$ K for type II PSC conditions. Temperature fluctuations with periods near τ_g contribute most heavily to the supersaturation $s = p_\xi/p_v - 1$ since fluctuations over very short times are quite small.

Departures from equilibrium in a PSC can be estimated by calculating the mean absolute supersaturation $|s|$. A simple estimate of $|s|$ is to simply multiply $|\Delta T|_g$ by the slope of vapor pressure versus temperature γ. However, the spectral density of the supersaturation can be found analytically under the assumption that the temperature fluctuations are small enough to linearize the vapor pressure $p_v \approx \gamma p_{v,0}(T - T_0)$. If the temperature does not cross the condensation point, then the partial pressure p_ξ of the condensing species satisfies $dp_\xi/dt = (p_v - p_\xi)/\tau_g$. For small temperature changes, these equations constitute a linear system. Consequently, the vapor pressure will respond independently to the Fourier components of the temperature fluctuations. Upon substitution, the supersaturation response to a temperature perturbation $\Delta T(t) = A_k e^{ikx}$ is $s(t) = \gamma A_k e^{ikx}[-iku\tau_g t/(1 + iku\tau_g t)]$. The spectrum of supersaturation follows as

$$\Phi_S = \gamma^2 \Phi_T k^2 u^2 \tau_g^2/(1 + k^2 u^2 \tau_g^2), \qquad (4)$$

where Φ_S is the spectral density of supersaturation and Φ_T is the spectral density of temperature. With a change of variables, Eq. (4) is familiar to electrical engineers in the context of white noise passing through an RC filter (Bracewell 1978). Figure 3 shows $d(s^2)/d(\ln(k)) = k\Phi_S$ evaluated for type I PSC conditions. By plotting $k\Phi_S$, the contributions of a frequency band to the variance of the saturation, which is s^2 (where s is the supersaturation), is visually equal to the area under the curve when using a logarithmic scale for the independent axis. For type I PSCs, most of the variance is due to wavelengths of ~100 km. For type II PSCs, most of the variance is due to wavelengths of ~10 km. Equation (4) is not accurate for frequencies less than about 0.02 km^{-1} because the linearity assumption fails for large-amplitude perturbations. However, these frequencies contribute little to the supersaturation.

The mean absolute value of the supersaturation can be solved analytically for the special case when $\Phi_T = bk^{-2}$ (Fig. 2a). In that case, Eq. (4) may be integrated over all wavenumbers to yield

$$\overline{|s|} \approx \gamma(b\tau_g u\pi/2)^{1/2}, \qquad (5)$$

where b is a scaling factor. Although the distribution is not necessarily Gaussian, $|s|$ is analogous to the standard deviation of supersaturation. For this special case, the deviation increases with the square root of the averaging time, just as in a random walk process. The values of $|s|$ in the remainder of this paper were obtained by numerically integrating Eq. (4) using the fit to Φ_T shown in Fig. 2. Our fit to Φ_T uses a slope of $-5/3$ except for a slope of -3 above 1 km^{-1} and an added Gaussian centered near 0.002 km^{-1}.

6. Discussion

a. PSC formation

Small but rapid temperature fluctuations dominate the rate of temperature change over the timescales that define the initial aerosol size distribution for both type I and type II PSCs. Typical cooling rates over the appropriate timescales are ≥ 50 K day^{-1}. The rates of temperature change considered here, which involve cooling and heating about a slower cooling trend, are not exactly analogous to those in most microphysical models, which usually presume monotonic cooling. An exception was the model of Drdla and Turco (1991), but that model did not include temperature fluctuations with periods less than a few hours.

Such large rates of temperature change mean that there is very little discrimination between condensation nuclei (CN). Wofsy et al. (1990) found that cooling rates of more than about 1 K day^{-1} produced particles too small for substantial sedimentation. Even with some particles serving as preferential nucleation sites, the observed rates of temperature change during PSC formation are too large for significant preferential activation of those particles. Some preliminary model calculations with mesoscale temperature fluctuations showed that all of the condensation nuclei are activated in most cases (L. Poole 1989, unpublished manuscript). Dye et al. (1990) found number densities of aerosols inside a type I PSC as large or larger than the CN number density outside the cloud. A possible explanation is that rapid temperature fluctuations as the cloud formed activated CN smaller than those measured by the CN instrument.

Metastable phases may exist in type I PSCs, such as mixed phases with sulfuric acid (Molina et al. 1993; Luo et al. 1994), liquid solutions (Hanson 1990), nitric acid dihydrate (Worsnop et al. 1993), other phases of nitric acid trihydrate (Koehler et al. 1992), or other mixtures of nitric acid and water (Marti and Mauersberger 1993). Rapid temperature fluctuations may promote metastable phases by suppressing annealing as the particles cool. A quantitative description of metastable phases in type I PSCs is beyond the scope of this paper. Indeed, the thermodynamic data required to calculate the rates at which aerosols convert between NAT and the various metastable phases of nitric acid and water have not been measured.

b. Established PSCs

Temperature fluctuations on short timescales will produce departures from equilibrium in established PSC. The transient supersaturations $|s|$ are surprisingly large, over 40% for type I PSC conditions and 3.5% for type II PSC conditions (Table 2). If anything, the fit to GASP data, taken at ~11-km altitudes, underestimates the supersaturations in PSCs because some mesoscale motions, such as gravity waves, amplify with altitude.

The Airborne Arctic Stratospheric Expedition (AASE) data show that temperature fluctuations cannot be the only factor controlling nitric acid vapor supersaturations in type I PSCs. Temperature fluctuations should result in supersaturation and subsaturation with about equal frequency, but AASE observations found that supersaturations with respect to NAT were much more common than subsaturations (Kawa et al. 1992). The nitric acid vapor pressure was probably controlled by some phase other than NAT (Hanson 1990; Koehler et al. 1992; Worsnop et al. 1993; Luo et al. 1994). Dye et al. (1992) and Larsen (1994) proposed that the formation of NAT or a metastable phase could depend on whether some or all of the sulfuric acid condensation nuclei were frozen instead of supercooled.

In 1989, Toon et al. pointed out a difficulty in modeling denitrification. Their calculations showed that denitrification was difficult to reproduce in a microphysical model, even with dehydration. The reason is that at synoptic-scale cooling rates, the nitric acid tends to be deposited on aerosols too small to sediment out. At that point, the nitric acid is locked into the aerosols and is unavailable for transfer to any larger particles that form later, even though it is thermodynamically favorable for the nitric acid to move to larger and more dilute particles. Turco et al. (1989) found that denitrification was possible only for a limited range of cooling rates. A later calculation by Toon et al. (1990) showed that an air parcel needed to spend over a week in a type I PSC for denitrification.

Because the rates of temperature change derived in this paper imply activation of large numbers of nuclei, the results presented here sharpen this difficulty in modeling denitrification. Besides activating fewer nuclei, another way of resolving the Toon et al. difficulty is the presence of metastable phases in type I PSCs. Any metastable phases will have higher equilibrium vapor pressures than NAT (Hanson and Mauersberger 1988). Since the characteristic times for aerosols to change size is inversely proportional to the partial pressure of the condensing species [Eq. (2)], the aerosol size distribution can change more rapidly if metastable phases are present.

There are considerable uncertainties in the estimates of transient departures from equilibrium vapor pressure. The estimates of 45% for type I and 3.5% for type II PSCs are based on a linear approximation. More accurate estimates could be made by imposing mesoscale temperature fluctuations on a detailed microphysical model. The observations for temperature fluctuations are also sparse in the lower stratosphere. There are only a handful of ER-2 flights parallel to the wind, and the large GASP dataset was collected at altitudes lower than PSCs. Finally, the characteristic temperature fluctuations used for this discussion are based on the average of the entire GASP dataset, even though there are

definite differences in the amplitude of temperature fluctuations above land and water (Gary 1989; Nastrom et al. 1987). Wind speeds are also systematically larger along the edge of the polar vortex than near the center. Besides the obvious difference that the edge of the polar vortex is warmer than the center, the difference in wind speed could cause a systematic difference in the microphysics of stratospheric dehydration and denitrification between the edge and center of the polar vortex. The one flight showing as an outlier in Fig. 3b did not have especially large temperature fluctuations. Instead, it was a flight along the edge of the vortex (20 February 1989) that encountered 50 m s^{-1} winds.

c. *Outside the stratosphere*

Dehydration at the tropical tropopause will have time constants similar to the PSC type II case shown here. Because most tropospheric clouds have more condensed and gas-phase mass, the timescales τ_p and τ_g are both shorter than in the stratosphere. For example, a calculation for the high tropical clouds reported in Knollenberg et al. (1993) yields $\tau_g \approx 12$ s and $|s| \approx 0.7\%$. These estimates are extremely uncertain because they involve extrapolating the spectral densities in Fig. 2, and the spectral densities may roll off at higher frequencies. The mean supersaturation becomes very small but the mass transfer to and from aerosols is faster at a given supersaturation. These two effects roughly cancel, so redistribution of mass to larger aerosols in high-altitude cirrus has a time constant comparable to that in type II PSCs. Politovich and Cooper (1988) calculated the spectral density of supersaturation due to turbulence in cumulus clouds. The mean departure from equilibrium was found to be a few tenths of a percent, which may be sufficient to broaden the droplet size distribution (Paluch 1971). It is likely that small-scale temperature fluctuations affect the activation of condensation nuclei in high-altitude cirrus. At lower altitudes, the importance of mesoscale fluctuations in the troposphere will be reduced because supersaturations produced by temperature fluctuations become much smaller than the saturation changes caused by solvent and Kelvin effects.

Jensen and Thomas (1994) found that temperature fluctuations caused by gravity waves significantly affect the albedo of noctilucent clouds. There, the effect is to suppress cloud formation because the exponential dependence of the H_2O vapor pressure versus temperature causes more evaporation in the warm phase of a wave than condensation in the cold phase. We have investigated the magnitude of this slowing in growth for type I PSCs by comparing the growth rate at constant temperature to a growth rate with Gaussian fluctuations. A standard deviation of 0.85 K was used to provide an upper limit to the effects away from mountain waves. The effect on the growth rate was significant only within about 1 K of the condensation point.

7. Conclusions

Mesoscale temperature fluctuations may have important effects on the microphysics of PSCs. The large rates of temperature change implied by observations suggest that most and perhaps all of the available CN will be activated when a PSC first forms. Once PSCs are formed, temperature fluctuations at different timescales have qualitatively different effects. At times longer than a characteristic relaxation time τ_g, condensation and evaporation can maintain supersaturations near zero, and temperature fluctuations result in changes in the partial pressure of the condensing species. At scales shorter than τ_g, the condensing species cannot respond quickly, and temperature fluctuations produce departures from equilibrium. Transient supersaturations have mean absolute values over 40% in type I PSCs and about 3.5% in type II PSCs. Previous models of PSC microphysics, which have considered only timescales much longer than τ_g, could not include the effects of these momentary supersaturations. One of the intentions of this paper is to stimulate detailed microphysical modeling that includes the different effects of temperature fluctuations on timescales both longer and shorter than τ_g.

A conventional view of denitrification requires that the activation and growth of a small fraction of condensation nuclei allows most of the nitric acid to reside on a small number of particles large enough to fall to lower altitudes. This view requires cooling rates slow enough for preferential activation of some nuclei. The hypothesis presented here is that cooling rates are usually large enough for the activation of all CN. Mass must then be redistributed to the most stable particles after the PSC has formed. Although this process is slow for NAT, changes in the aerosol size distribution after the PSC is formed are more rapid if type I PSCs are composed of a metastable phase rather than NAT. Because it does not allow time for annealing, a rapid cooling rate could promote the formation of a large number of metastable particles and subsequent mass transfer to larger, more stable particles.

Acknowledgments. We thank Greg Nastrom for pulling out some of the GASP data for use in this paper. A portion of the research described in this publication was carried out by the Jet Propulsion Laboratory, California Institute of Technology, under a contract with the National Aeronautics and Space Administration.

REFERENCES

Bacmeister, J. T., and B. L. Gary, 1990: Small-scale waves encountered during AASE. *Geophys. Res. Lett.*, **17**, 349–352.

Bracewell, R. N., 1978: *The Fourier Transform and Its Applications.* McGraw-Hill, 444 pp.

Denning, R. F., S. L. Guidero, G. S. Parks, and B. L. Gary, 1989: Instrument description of the airborne microwave temperature profiler. *J. Geophys. Res.*, **94**, 16 757–16 765.

Drdla, K., and R. P. Turco, 1991: Denitrification through PSC formation: A 1-D model incorporating temperature oscillations. *J. Atmos. Chem.*, **12,** 319–366.

Dye, J. E., B. W. Gandrud, D. Baumgardner, K. R. Chan, G. V. Ferry, M. Loewenstein, K. K. Kelly, and J. C. Wilson, 1990: Observed particle evolution in the polar stratospheric cloud of January 24, 1989. *Geophys. Res. Lett.*, **17,** 413–416.

——, D. Baumgardner, B. W. Gandrud, S. R. Kawa, K. K. Kelly, M. Loewenstein, G. V. Ferry, K. R. Chan, and B. L. Gary, 1992: Particle size distributions in Arctic polar stratospheric clouds, growth and freezing of sulfuric acid droplets, and implications for cloud formation. *J. Geophys. Res.*, **97,** 8015–8034.

Gage, K. S., and G. D. Nastrom, 1986: Spectrum of atmospheric vertical displacements and spectrum of conservative scalar passive additives due to quasi-horizontal atmospheric motions. *J. Geophys. Res.*, **92,** 13 211–13 216.

Gary, B. L., 1989: Observational results using the microwave temperature profiler during the Airborne Antarctic Ozone Experiment. *J. Geophys. Res.*, **94,** 11 223–11 231.

Hanson, D. R., 1990: The vapor pressures of supercooled HNO_3/H_2O solutions. *Geophys. Res. Lett.*, **17,** 421–423.

——, and K. Mauersberger, 1988: Laboratory studies of the nitric acid trihydrate: Implications for the South Polar stratosphere. *Geophys. Res. Lett.*, **15,** 855–858.

Jensen, E. J., and G. E. Thomas, 1994: Numerical simulations of the effects of gravity waves on noctilucent clouds. *J. Geophys. Res.*, **99,** 3421–3430.

Kawa, S. R., D. W. Fahey, K. K. Kelly, J. E. Dye, D. Baumgardner, B. W. Gandrud, M. Loewenstein, F. V. Ferry, and K. R. Chan, 1992: The Arctic polar stratospheric cloud aerosol: Aircraft measurements of reactive nitrogen, total water, and particles. *J. Geophys. Res.*, **97,** 7925–7938.

Knollenberg, R. G., K. Kelly, and J. C. Wilson, 1993: Measurements of high number densities of ice crystals in the tops of tropical cumulonimbus. *J. Geophys. Res.*, **98,** 8639–8664.

Koehler, B. G., A. M. Middlebrook, and M. A. Tolbert, 1992: Characterization of model polar stratospheric cloud films using Fourier transform infrared spectroscopy and temperature programmed desorption. *J. Geophys. Res.*, **97,** 8065–8074.

Laprise, R., 1992: The resolution of global spectral models. *Bull. Amer. Meteor. Soc.*, **73,** 1453–1454.

Larsen, N., 1994: The impact of freezing of sulfate aerosols on the formation of polar stratospheric clouds. *Geophys. Res. Lett.*, **21,** 425–428.

Luo, B. P., S. L. Clegg, T. Peter, R. Müller, and P. J. Crutzen, 1994: HCl solubility and liquid diffusion in aqueous sulfuric acid under stratospheric conditions. *Geophys. Res. Lett.*, **21,** 49–52.

Marti, J., and K. Mauersberger, 1993: Laboratory simulations of PSC particle formation. *Geophys. Res. Lett.*, **20,** 359–362.

Molina, M. J., R. Zhang, P. J. Woodbridge, J. R. McMahon, J. E. Kim, H. Y. Chang, and K. D. Beyer, 1993: Physical chemistry of the $H_2SO_4/HNO_3/H_2O$ system: Implications for polar stratospheric clouds. *Science,* **261,** 1418–1423.

Murphy, D. M., 1989: Time offsets and power spectra of the ER-2 data set from the 1987 Airborne Antarctic Ozone Experiment. *J. Geophys. Res.*, **94,** 16 737–16 748.

Nastrom, G. D., and K. S. Gage, 1985: A climatology of atmospheric wavenumber spectra of wind and temperature observed by commercial aircraft. *J. Atmos. Sci.*, **42,** 950–960.

——, W. H. Jasperson, and K. S. Gage, 1986: Horizontal spectra of atmospheric tracers measured during the Global Atmospheric Sampling Program. *J. Geophys. Res.*, **91,** 13 201–13 209.

——, D. C. Fritts, and K. S. Gage, 1987: An investigation of terrain effects on the mesoscale spectrum of atmospheric motions. *J. Atmos. Sci.*, **44,** 3087–3096.

Paluch, I. R., 1971: A model for cloud droplet growth by condensation in an inhomogeneous medium. *J. Atmos. Sci.*, **28,** 629–639.

Politovich, M. K., and W. A. Cooper, 1988: Variability of the supersaturation in cumulus clouds. *J. Atmos. Sci.*, **45,** 1651–1664.

Salawitch, R. J., G. P. Gobbi, S. C. Wofsy, and M. B. McElroy, 1989: Denitrification in the Antarctic stratosphere. *Nature,* **339,** 525–527.

Scott, G. S., T. P. Bui, K. R. Chan, and S. W. Bowen, 1990: The meteorological measurement system on the NASA ER-2 aircraft. *J. Atmos. Oceanic Technol.*, **7,** 525–540.

Tolstov, G. P., 1962: *Fourier Series.* Dover, 336 pp.

Toon, O. B., R. P. Turco, J. Jordan, J. Goodman, and G. Ferry, 1989: Physical processes in polar stratospheric ice clouds. *J. Geophys. Res.*, **94,** 11 359–11 380.

——, ——, and P. Hamill, 1990: Denitrification mechanisms in the polar stratosphere. *Geophys. Res. Lett.*, **17,** 445–448.

Turco, R. P., O. V. Toon, and P. Hamill, 1989: Heterogeneous physicochemistry of the polar ozone hole. *J. Geophys. Res.*, **94,** 16 493–16 510.

Wagner, P. E., 1982: Aerosol growth by condensation. *Aerosol Microphysics II,* W. H. Marlow, Ed., Springer-Verlag, 129–178.

Wofsy, S. C., G. P. Gobbi, R. Salawitch, and M. B. McElroy, 1990: Nucleation and growth of $HNO_3 \cdot 3H_2O$ particles in the polar stratosphere. *J. Atmos. Sci.*, **47,** 2004–2012.

Worsnop, D. W., L. E. Fox, M. S. Zahnhiser, and S. C. Wofsy, 1993: Vapor pressures of solid hydrates of nitric acid: Implications for polar stratospheric clouds. *Science,* **259,** 71–74.